Translational Evidence for Dopaminergic Rewiring of the Basal Ganglia in Persons with Schizophrenia

*Philip N. Tubiolo, MS[1,2,3], *John C. Williams, PhD[1,2,4], Roberto B. Gil, MD[2,5,6], Clifford Cassidy, PhD[2], Natalka K. Haubold, BA[2], Yash Patel, MS[2], Sameera K. Abeykoon, PhD[2], Zu Jie Zheng, BS[2,7], Dathy T. Pham[2,8], Najate Ojeil, PhD, MPH[5,6], Kelly Bobchin, BA[2], Eilon B. Silver-Frankel, BS[2], Greg Perlman, PhD[2], Jodi J. Weinstein, MD[2,5,6], Christoph Kellendonk, PhD[5,6,9], Guillermo Horga, MD, PhD[5,6], Mark Slifstein, PhD[2,5,6], Anissa Abi-Dargham, MD[1,2,5,6,10] & Jared X. Van Snellenberg, PhD[1,2,5,6,11]

*These authors contributed equally to this work

[1]Department of Biomedical Engineering, Stony Brook University, Stony Brook, NY 11794;
[2]Department of Psychiatry and Behavioral Health, Renaissance School of Medicine at Stony Brook University, Stony Brook, NY 11794;
[3]Scholars in BioMedical Sciences Training Program, Renaissance School of Medicine at Stony Brook University, Stony Brook, NY 11794;
[4]Medical Scientist Training Program, Renaissance School of Medicine at Stony Brook University, Stony Brook, NY 11794;
[5]Department of Psychiatry, Columbia University Vagelos College of Physicians and Surgeons, New York-Presbyterian / Columbia University Irving Medical Center, New York, NY 10032;
[6]New York State Psychiatric Institute, New York, NY 10032;
[7]College of Medicine, State University of New York Downstate Health Sciences University, Brooklyn, NY 11203;
[8]Department of Neurobiology and Behavior, Cornell University, Ithaca, NY 14853;
[9]Department of Molecular Pharmacology & Therapeutics, Vagelos College of Physicians and Surgeons, New York-Presbyterian / Columbia University Irving Medical Center, New York, NY 10032;
[10]Department of Radiology, Renaissance School of Medicine at Stony Brook University, Stony Brook, NY 11794;
[11]Department of Psychology, Stony Brook University, Stony Brook, NY 11794.

CORRESPONDING AUTHOR:
Jared X. Van Snellenberg
101 Nicolls Rd
Health Sciences Center 10-087J
Stony Brook, NY 11794
Jared.VanSnellenberg@stonybrookmedicine.edu

Key Points

Question: Do unmedicated persons with schizophrenia display dopamine-related alterations in basal ganglia functional connectivity?

Findings: In this case-control study, we observed hyperconnectivity between the dorsal caudate and globus pallidus externus during a working memory task in unmedicated persons with schizophrenia. This phenotype was associated with worse task performance and measures of subcortical dopamine function obtained via neuromelanin-sensitive magnetic resonance imaging and [^{11}C]-(+)-PHNO positron emission tomography.

Meaning: This study provides in-vivo evidence that dopaminergic rewiring of the basal ganglia may be a neurodevelopmental mechanism for working memory deficits in schizophrenia, emulating findings from a transgenic mouse model of striatal dopamine dysfunction.

Abstract

Importance: In prior work, a transgenic mouse model of the striatal dopamine dysfunction observed in persons with schizophrenia (PSZ) exhibited dopamine-related neuroplasticity in the basal ganglia. This phenotype has never been demonstrated in human PSZ.

Objective: To identify a specific dopamine-related alteration of basal ganglia connectivity via task-based and resting-state functional magnetic resonance imaging (fMRI), neuromelanin-sensitive MRI (NM-MRI), and positron emission tomography (PET), in unmedicated PSZ.

Design: This case-control study of unmedicated PSZ and healthy controls (HC) occurred between November 2014 and June 2018, with analyses performed between April 2023 and February 2025.

Setting: fMRI and NM-MRI were collected at New York State Psychiatric Institute. [^{11}C]-(+)-PHNO PET was collected at Yale University.

Participants: Participants were aged 18-55, and demographically matched. PSZ were antipsychotic drug-naïve or drug-free for at least three weeks prior to recruitment.

Main Outcomes and Measures: 1) task-state and resting-state functional connectivity (FC) between dorsal caudate (DCa) and globus pallidus externus (GPe), 2) NM-MRI contrast ratio in substantia nigra voxels associated with psychotic symptom severity, and 3) baseline and amphetamine-induced change in [^{11}C]-(+)-PHNO binding potential in DCa.

Results: 37 PSZ (mean±SD age, 32.7±12.7 years, 29.7% female) and 30 HC (32.5±9.7 years, 26.7% female) underwent resting-state fMRI; 29 PSZ (33.4±12.7 years, 31% female) and 29 HC (32.4±9.7 years, 31% female) underwent working memory task-based fMRI. 22 PSZ (35.1±13.9 years, 36.4% female) and 20 HC (29.4±8.5 years, 35% female) underwent NM-MRI. 7 PSZ (23.1±6.3 years, 57.1% female) and 4 HC (31.5±11.9 years, 25% female) underwent [^{11}C]-(+)-PHNO PET with amphetamine challenge. PSZ displayed elevated task-state FC (0.11±0.10 versus 0.05±0.09 in HC; P=0.0252), which was associated with increased NM-MRI contrast

ratio (β* [SE] = 0.40 [0.17]; *P*=0.023), decreased baseline D2 receptor availability (β* [SE] = -0.45 [0.17]; *P*=0.039), greater amphetamine-induced dopamine release (β* [SE] = -0.82 [0.27]; *P*=0.021), and worse task performance (β* [SE] = -0.31 [0.13]; *P*=0.020).

Conclusions and Relevance: This study provides in-vivo evidence of a dopamine-associated neural abnormality of DCa and GPe connectivity in unmedicated PSZ. This phenotype suggests a potential neurodevelopmental mechanism of working memory deficits in schizophrenia, representing a critical step towards developing treatments for cognitive deficits.

Abbreviations

ANTs, Advanced Normalization Tools;

BGTC, basal ganglia-thalamo-cortical;

BOLD, blood-oxygen-level-dependent;

BP_{ND}, binding potential (non-displaceable);

CIFTI, connectivity informatics technology initiative;

CNR, contrast ratio;

D1R, dopamine D1 receptor;

D2R, dopamine D2 receptor;

D2R-OE, dopamine D2 receptor overexpressing;

DCa, dorsal caudate;

DLPFC, dorsolateral prefrontal cortex;

DOPA, dihydroxyphenylalanine;

FC, functional connectivity;

FDR, false discovery rate;

fMRI, functional magnetic resonance imaging;

GABA, gamma-aminobutyric acid;

GEV-DV, generalized extreme value DVARS;

GPe, globus pallidus externus;

GPi, globus pallidus internus;

HC, healthy control;

HRF, hemodynamic response function;

IBZM, iodobenzamide;

IQR, interquartile range;

K_{ir}, inwardly rectifying potassium;

MNI, Montreal Neurologic Institute;

MP, motion parameter;

MSN, Medium spiny neuron;

NM-MRI, neuromelanin-sensitive magnetic resonance imaging;

NYSPI, New York State Psychiatric Institute;

PANSS, positive and negative syndrome scale;

PET, positron emission tomography;

PHNO, 4-propyl-9-hydroxynaphthoxazine;

PSZ, persons with schizophrenia;

ROI, region of interest;

RS, resting-state;

rs-FC, resting-state functional connectivity;

SD, standard deviation;

SE, standard error;

SN, substantia nigra;

SOT, self-ordered working memory task;

SPM12, Statistical Parametric Mapping 12;

STN, subthalamic nucleus;

ts-FC, task-state functional connectivity;

TE, echo time;

TR, repetition time;

VTA, ventral tegmental area;

WM, working memory

1. Introduction

Evidence of striatal dopamine dysfunction in persons with schizophrenia (PSZ) is among the most robust and consistently replicated findings in the neurobiology of schizophrenia. Studies with [^{18}F]DOPA show elevated presynaptic striatal dopamine synthesis in medication-naïve and medication-free PSZ[1-7], as well as individuals at clinical high risk for schizophrenia[8-10]. Studies using radiolabeled dopamine D2 receptor (D2R) antagonists [^{123}I]IBZM or [^{11}C]raclopride show increased amphetamine-induced tracer displacement in striatum in PSZ[11-13], while depletion of dopamine with alpha-methyl-para-tyrosine results in increased tracer binding in PSZ[14,15], suggesting PSZ exhibit higher occupancy of D2 receptors due to higher synaptic levels of DA, consistent with increased presynaptic availability and release of dopamine. These findings spurred the development of a transgenic mouse model to mimic this abnormality and study the neurophysiological consequences of excess striatal D2R stimulation. D2R overexpressing (D2R-OE) mice have selectively increased expression of D2Rs in the caudate-putamen, with expression temporally controllable via doxycycline[16]. D2R-OE mice display performance deficits in a delayed non-match-to-sample T-maze task that persist even if D2R overexpression is halted in adulthood[16], suggesting a neurodevelopmental cognitive deficit reminiscent of those seen in human PSZ[17-19].

D2R-OE mice also display striking neuroplasticity within the basal ganglia-thalamo-cortical (BGTC) circuit[20], which plays critical modulatory roles in motor, limbic, and cognitive functioning[21,22]. This circuit is comprised of two functionally opposed pathways, the “direct” pathway and the “indirect” pathway (**Figure 1**). While these pathways were initially thought to be anatomically segregated, tracing studies in rats and monkeys demonstrate that some direct pathway D1R-expressing medium spiny neurons (MSNs), which project to the globus pallidus internus (GPi; entopeduncular nucleus in rodents) and substantia nigra (SN) pars reticulata, actually bifurcate and send additional collaterals to the globus pallidus externus (GPe)[23-26]; these are termed “bridging collaterals,” as they bridge the direct and indirect pathways[20]. D2R-

OE mice exhibit a highly plastic increase in bridging collateral density, which decreased when the overexpression was halted by doxycycline in adult animals but returned to elevated levels when doxycycline was removed. Haloperidol, a D2 antagonist antipsychotic, also reduces bridging collateral density in D2R-OE and wildtype animals, while D2R knockdown mice exhibit dose-dependent reductions in bridging collateral density[20], demonstrating that D2R stimulation in the striatum is a causal mechanism of bridging collateral density. Functionally, this plasticity is hypothesized to be a homeostatic mechanism regulating the balance of excitability in the direct and indirect pathways: paradoxically, upregulation of D2Rs results in downregulation of inwardly-rectifying potassium (K_{ir}) channels[27], resulting in *increased* excitability of indirect pathway MSNs (in spite of D2Rs themselves being inhibitory). Thus, increased bridging collaterals from the direct pathway may counter increased indirect pathway excitability and restore the overall balance of thalamic excitation and inhibition. However, given that cognitive deficits persist in D2R-OE mice after the reversal of D2R overexpression, further neurodevelopmental abnormalities with the BGTC circuit may be present as a result of this compensatory mechanism. Notably, bridging collateral density in D2R-OE mice was greatest between associative striatum (medial caudate-putamen) and medial pallidum, which receives input from associative cortical regions such as the dorsolateral prefrontal cortex (DLPFC)[20,28]. Similarly, higher-resolution PET imaging studies in human PSZ have shown greater baseline occupancy of D2Rs in the dorsal caudate (DCa), and more broadly in the associative striatum, as compared to ventral and sensorimotor striatum[14,29,30].

Overall, these findings provide robust evidence of neuroplasticity of striatopallidal projections in response to D2R density in a transgenic mouse developed to mimic striatal dopamine dysfunction in PSZ. Here, we sought to translate these findings to human patients, hypothesizing that if this compensatory response to D2R overstimulation occurs in PSZ, it should be detectable as altered functional connectivity (FC) between the striatum (specifically DCa) and the GPe. However, available evidence also suggests that: 1) any alteration in FC may

only be observable in unmedicated PSZ, as D2R antagonists reduce the density of bridging collaterals in rodents; 2) while altered anatomical connectivity should alter DCa-GPe FC, the expected direction of change is somewhat unclear—although striatal MSNs are GABA-ergic and thus inhibitory, net inhibition of a region is still metabolically demanding and can increase functional Magnetic Resonance Imaging (fMRI) Blood Oxygen Level-Dependent (BOLD) signal[31,32]; and finally, 3) because striatal MSNs are hyperpolarized at rest, with low baseline firing rates[33,34], any observed change in FC may only be apparent under conditions in which the affected basal ganglia circuitry is actively processing information and MSNs are activated. Consequently, we conducted an FC MRI study of unmedicated PSZ in both a resting state and during the performance of a working memory (WM) task that we have shown robustly activates the DCa and other striatal regions[35], in order to test whether we could observe altered DCa-GPe connectivity during rest or task that could inform our hypothesis that unmedicated PSZ have increased bridging collateral density.

Given the interconnected nature of the BGTC circuit, we also chose to implement a network modeling approach to calculating FC between regions. This addresses the “third variable” problem, in which altered FC between regions could be driven by a third region that is not accounted for in the model. For example, apparent altered striato-pallidal connectivity could be driven by altered pallido-thalamic or thalamo-cortical connectivity that then propagates through the network. Our approach calculates FC as a partial correlation controlling for timeseries in regions of interest (ROIs) outside each given ROI pair, a straightforward method that reliably distinguishes between direct and indirect network connections in simulated and *in vivo* data[36-38] .

In addition, many of our participants were also enrolled in other neuroimaging studies, which included studies of dopamine function that could further inform whether altered FC might be driven by striatal dopamine dysfunction. Thus, in two subsets of our sample, we also report on the relationship between DCa-GPe FC and dopamine function measured via 1) neuromelanin-sensitive MRI (NM-MRI) of the SN (an indirect measure of long-term dopamine turnover that is

correlated with psychotic symptoms[39,40]) and; 2) Positron Emission Tomography (PET) with the D2/3 agonist radiotracer [^{11}C]-(+)-PHNO [30,41,42] and an amphetamine challenge. Finally, we also conducted exploratory analyses examining the relationship between DCa-GPe connectivity and WM task performance and positive and negative symptoms in PSZ.

2. Methods

2.1. Overview

This is a case-control study of unmedicated PSZ and healthy controls (HC) aged 18-55 years old and demographically matched on age, parental socioeconomic status, race, and ethnicity. All procedures occurred at the New York State Psychiatric Institute (NYSPI) except PET scanning, which occurred at Yale University. PSZ were considered unmedicated if they were antipsychotic-naïve or antipsychotic-free for at least three weeks prior to recruitment. All participants were free of major neurological disorders, current substance use disorders, and psychiatric disorders other than schizophrenia, schizophreniform disorder, or schizoaffective disorder. Full inclusion and exclusion criteria are described in the **Supplementary Methods.** All procedures were approved by the NYSPI and Yale Institutional Review Boards.

2.2. Participants

Thirty-seven PSZ and 30 HC completed RS fMRI, with a subset of 29 PSZ and 29 HC completing task-based fMRI. Additionally, 22 PSZ and 20 HC who performed task-based fMRI underwent NM-MRI. Finally, a smaller subset of 7 PSZ and 4 HC underwent [^{11}C]-(+)-PHNO PET with amphetamine challenge. Participants underwent several clinical and demographic assessments described in the **Supplementary Methods**. RS fMRI data and NM-MRI data from a subset of these participants has been previously analyzed and reported on elsewhere[39,43].

2.3. Neuroimaging Procedures

MRI equipment, sequences, and processing are described in detail in the **Supplementary Methods.** Briefly, in addition to standard structural sequences, we collected multiband fMRI

scans with 2 mm isotropic voxel resolution for approximately 30 minutes each for RS and task-state FC. We employed the self-ordered working memory task[35,44] (SOT; see **Figure S1** for task schematic), and neural responses to task-events were modeled as per our prior work[35,45]. The WM task fMRI data were then residualized with respect to the modeled task-evoked activation to distinguish task-state FC (ts-FC) from task-related coactivation[46,47]. Preprocessing was conducted with the Human Connectome Project Minimal Preprocessing Pipeline[48], version 4.2.0, followed by established FC-specific processing methods from our prior work[49]. Finally, ts-FC used only "task-on" volumes, which were identified as all volumes beginning two seconds after each task block onset and ending four seconds after the final trial of the block (to account for the initial delay in hemodynamic response and gradual return to baseline)[50].

In order to use network modeling to estimate DCa-GPe connectivity, we identified a set of regions in the BGTC circuit with established roles in cognitive and associative functions. ROIs included the mediodorsal nucleus (MD), DCa, GPe, GPi, SN, and DLPFC (see **Supplementary Methods** for identification procedures). We omitted the subthalamic nucleus from this network model, despite its importance in the indirect pathway, due to its small size and the lack of a reliable localization technique. **Figure S2** displays the surface-based DLPFC ROI, and **Figure S3** displays the probability density of all volumetric subcortical ROIs.

NM-MRI, collected in a subset of our participants, used acquisition parameters and processing procedures described elsewhere[39] and in the **Supplementary Methods**. Our NM-MRI outcome measure was the average contrast ratio (CNR) extracted from *a priori* voxels within an overinclusive mask of the SN and ventral tegmental area (VTA) whose CNR is correlated with both psychosis severity in PSZ (measured as PANSS Positive subscale score[51]) and subclinical positive symptom severity in persons at clinical high risk for developing a psychotic disorder[39,40].

PET data were acquired using procedures described elsewhere[52] and in the **Supplementary Methods**. Final outcome measures included both baseline binding potential (BP_{ND}) and the fractional change in BP_{ND} following amphetamine administration,

$\frac{BP_{ND}(\text{post-amph.})}{BP_{ND}(\text{baseline})} - 1$ (ΔBP_{ND}), within a hand-drawn DCa ROI.

2.4. Statistical Analysis

Effect sizes for group differences were calculated using Hedges' *g*[53] or Cramér's *V*[54], as appropriate. Group differences in PANSS sub-scores, SOT performance[44] and the proportion of correct responses in the SOT were assessed using Mann-Whitney U-tests.

Group differences in ROI pair FC were assessed via independent samples t-tests or Mann-Whitney U-tests, dependent on data normality (determined via Lilliefors test). The primary hypothesis investigating group differences in DCa-GPe rs-FC and ts-FC was assessed for significance at α=0.05 with Dunn–Šidák correction[55] for two comparisons. Post-hoc tests of group connectivity differences between all other ROI pairs were assessed at α=0.05 with false discovery rate (FDR) correction[56] across all tests. As a supplementary analysis, we also assessed for group differences in DCa-GPe ts-FC using a robust multivariable linear regression with age and biological sex as covariates.

Associations between DCa-GPe ts-FC and either SOT performance (measured as WM capacity *k*[44]), average NM-MRI signal, [^{11}C]-(+)-PHNO baseline BP_{ND}, or ΔBP_{ND} were assessed via robust multivariable linear regression with age, biological sex, and diagnosis as covariates; associations with PANSS positive and negative symptoms scores were assessed in PSZ only, using the same covariates above except diagnosis. All betas are reported as standardized regression coefficients β^*.

3. Results

3.1. Demographics

Thirty-seven PSZ and 30 HC completed at least two runs of resting-state fMRI (N=67), with zero participants excluded for excess motion. Additionally, 29 PSZ and 29 HC completed at least two runs of task-based fMRI (N=58), after excluding four participants due to excess motion. A summary table of demographic information for each cohort is shown in **Table 1**.

Group differences in SOT working memory capacity (*k*) and the proportion of correct responses are shown in **Figure S4**. The median [IQR] SOT *k* for HC and PSZ were 5.92 [1.61] and 4.73 [3.42], respectively (*P*=0.127). The median [IQR] proportion of correct responses in HC and PSZ were 0.94 [0.08] and 0.88 [0.23], respectively (*P*=0.139).

3.2. Resting-state and Task-state Functional Connectivity

Between DCa and GPe (ROIs shown in **Figure 2A, B**), no significant group difference in resting-state functional connectivity (rs-FC) was observed (median [IQR] of 0.05 [0.16] in HC and 0.08 [0.12] in PSZ, *P*=0.233; **Figure 2C**). PSZ displayed elevated ts-FC between DCa and GPe relative to HC that survives Dunn–Šidák correction (mean [SD] of 0.05 [0.09] in HC and 0.11 [0.10] in PSZ, *P*=0.0252**; Figure 2D**). This group difference in ts-FC remained statistically significant when controlling for age and biological sex via robust regression (β* [SE] = 0.27 [0.14], *P*=0.048**; Table S1**).

Within other direct connections in the BGTC circuit, HC displayed greater MD-DCa rs-FC than PSZ (mean [SD] of 0.27 [0.12] in HC and 0.17 [0.15] in PSZ, *P*=0.005**; Figure S5H**). No significant differences in ts-FC were observed following FDR correction (**Figure S6**), although MD-DLPFC ts-FC was elevated in PSZ before correction.

3.3. Neuromelanin-Sensitive MRI

The average NM-MRI contrast-ratio map across participants is shown in **Figure 3A**. In the *a priori* psychosis-associated voxels[39,40], average NM-MRI contrast was positively associated with DCa-GPe ts-FC (β* [SE] = 0.40 [0.17], *P*=0.023**; Figure 3B**, **Table S2**).

3.4. [^{11}C]-(+)-PHNO Positron Emission Tomography

In the subset of seven PSZ and four HC that completed both WM task-based fMRI and [^{11}C]-(+)-PHNO PET, elevated DCa-GPe ts-FC was found to be significantly negatively associated with DCa baseline D2R availability, measured as [^{11}C]-(+)-PHNO BP_{ND} (β* [SE] = -0.45 [0.17], *P*=0.039; **Figure 3C, Table S3**). Additionally, greater DCa-GPe ts-FC was associated with more negative DCa ΔBP_{ND} (β* [SE] = -0.82 [0.27], *P*=0.021; **Figure 3D**, **Table S3**), where a more negative ΔBP_{ND} indicates greater fractional decrease in BP_{ND} following amphetamine administration.

3.5. Associations between Task-state Functional Connectivity and Symptomatology

Elevated DCa-GPe ts-FC was associated with lower SOT *k* across all participants (β* [SE] = -0.31 [0.13], *P*=0.020**; Figure 4A**, **Table S4**). In PSZ, no significant associations were observed between DCa-GPe ts-FC and PANSS positive symptom score (β* [SE] = -0.39 [0.21], *P*=0.068**; Figure 4B, Table S5**) or PANSS Negative symptom score (β* [SE] = -0.20 [0.23], *P*=0.389**; Figure 4C, Table S5**).

4. Discussion

The results presented here support our hypothesis of specifically altered dorsal caudate-globus pallidus externus (DCa-GPe) connectivity in unmedicated persons with schizophrenia, which we developed *a priori* based on evidence of neuroanatomical reorganization of this circuitry in the dopamine D2 receptor overexpressing (D2R-OE) mouse model[16,20,57,58] of striatal dopamine dysfunction in schizophrenia. Notably, our findings also provide multiple lines of evidence that this alteration is associated with striatal dopamine dysfunction, in addition to working memory (WM) deficits, consistent with the dopamine dysfunction and WM deficits in the D2R-OE mice that spurred this investigation. While rs-FC findings were negative, we demonstrated DCa-GPe hyperconnectivity in unmedicated PSZ during the performance of a WM task, a condition we tested specifically because striatal MSNs are relatively quiet at resting state due to a negative intrinsic resting membrane potential. This may prevent the detection of

altered fMRI connectivity unless receiving stimulation from cortical and thalamic inputs during cognitive processing. Critically, the full set of secondary analyses are also entirely consistent with our hypotheses, with significant correlations between DCa-GPe ts-FC and WM as well as all dopaminergic outcome measures collected in our sample, and with DCa-GPe ts-FC being specifically elevated, rather than part of a broader alteration of ts-FC throughout the BGTC network (see **Figure S6**). While our findings cannot directly establish that elevated DCa-GPe ts-FC in PSZ is a result of upregulated bridging collaterals from D1R-containing MSNs to the GPe, we developed a direct, falsifiable, experimental test of the hypothesis that unmedicated PSZ exhibit a similar upregulation of bridging collaterals as has been observed in D2R-OE mice, and found formal support for this conclusion.

Our findings suggest a pivotal role of subcortical dopamine dysfunction in striato-pallidal neuronal reorganization. NM-MRI signal in the SN and VTA is a proxy measure of long-term dopamine turnover (unless neuronal cell death has occurred, e.g. in Parkinson's disease)[40,59,60] that has been shown to be associated with the severity of psychotic symptoms[39,61]. Elevated nigral NM signal suggests upregulated dopamine turnover in nigral cell bodies, which likely results in elevated presynaptic availability and release in striatum[62], a well-established finding in PSZ linked to psychosis severity[11,14,15,29,63-65]. Although observed in a small, preliminary sample, our finding that individuals who show stronger dopamine release following amphetamine challenge have more greatly elevated DCa-GPe connectivity directly supports this interpretation. Similarly, decreased baseline D2R availability was also associated with DCa-GPe hyperconnectivity, consistent with increased baseline availability of dopamine in the DCa that competes with radiotracer binding, resulting in lower BP_{ND} in these participants. However, we cannot rule out the possibility that lower D2R density in DCa also contributes to lower BP_{ND}.

Finally, we found that elevated DCa-GPe ts-FC is associated with poorer WM task performance, analogous to the performance deficits in a delayed non-match to sample T-maze in D2R-OE mice. Given that these deficits in D2R-OE mice remained when upregulation of

DCa-GPe bridging collaterals was normalized via D2R antagonist antipsychotic administration, this finding suggests that DCa-GPe hyperconnectivity may be a state-dependent predictor of the neurodevelopmental impact of persistent dopamine dysfunction in PSZ prior to becoming medicated. That is, unmedicated PSZ with more severe subcortical dopamine dysfunction develop greater bridging collateral density between DCa and GPe, thus driving further BGTC circuit reorganization that directly disrupts the maintenance of internal representations of task stimuli in prefrontal cortical regions; e.g., via effects on D1R function in DLPFC, which is thought to be disrupted in SCZ[66], critical for WM[67], and altered in D2R-OE mice[16,27]. A potential mechanism for this resulting cortical dysfunction is the persistent functional abnormalities that have been shown to exist in dopamine neurons of D2R-OE mice, particularly decreased phasic activity and neuronal recruitment under WM task demands[68,69]. These abnormalities may not be normalized via antipsychotic medication given after their development, resulting in the persistence of WM deficits.

In summary, this study provides in-vivo translational evidence of a specific neural abnormality between the DCa and GPe in unmedicated PSZ, emulating findings from the D2R-OE transgenic mouse model. This abnormality was observed in the form of elevated FC during WM task engagement and was associated with poor WM task performance and disrupted subcortical dopaminergic function measured by two imaging modalities. Future work should aim to demonstrate structural evidence of altered DCa-GPe anatomical connectivity, as well as examine the role of D2R antagonist antipsychotic medication in the normalization of the phenotype. Nevertheless, these results build on a rich literature implicating subcortical dopaminergic dysfunction in the pathophysiology of SCZ to suggest a neurodevelopmental mechanism of WM deficits in PSZ, a crucial step towards the development of novel therapeutic targets and treatments.

5. Data and Code Availability

All data and analysis code used in the preparation of this manuscript can be made available upon request to the corresponding author through a formal data sharing agreement.

6. Funding

Research reported in this publication was supported by the National Institute of Mental Health of the National Institutes of Health (NIH) under award numbers K01MH107763 to J.X.V.S., K23MH101637 to G.H., R01MH109635 to A.A-D., R01MH124858 to C.K., F30MH122136 to J.C.W, and K23MH115291 to J.J.W. P.N.T. was supported by the Stony Brook University Scholars in Biomedical Sciences Program (NIH Award No. T32GM148331; PI: Dr. Styliani-Anna [Stella] E. Tsirka). J.C.W. was also supported by a Research Supplement to Promote Diversity in Health-Related Research (3R01MH120293-04S1) and by the Stony Brook University Medical Scientist Training Program (Award No. T32GM008444; Principal Investigator: Dr. Michael A. Frohman). The Stony Brook high-performance SeaWulf computing system was supported by National Science Foundation (NSF) Award Nos. 1531492 (PI: Dr. Robert Harrison; co-PI: Dr. Yuefan Deng) and 2215987 (PI: Dr. Robert Harrison; co-PIs: Dr. Yuefan Deng, Dr. Eva Siegmann, and David Cyrille), and matching funds from the Empire State Development's Division of Science, Technology and Innovation (NYSTAR) program contract C210148. The Stony Brook University Social, Cognitive, and Affective Neuroscience (SCAN) Center was supported by NSF Award No. 0722874 (PI: Dr. Turhan Canli). This content is solely the responsibility of the authors and does not necessarily represent the official views of the NIH, NSF, or NYSTAR.

7. Competing Interests

Drs. Cassidy and Horga are inventors on patents for the analysis of NM-MRI, licensed to Terran Biosciences, Inc., but have received no royalties. Drs. Cassidy and Horga have an investigator-initiated sponsored research agreement and a licensing agreement with Terran Biosciences, Inc. Dr. Slifstein reports having served as a paid consultant for Neurocrine

Biosciences, Inc. and for Yale University. Dr. Abi-Dargham received consulting fees from Neurocrine Biosciences, Inc., from Abbvie, Inc., and from MapLight Therapeutics, Inc. Dr. Abi-Dargham holds stock options in Herophilus, Inc. and in Terran Biosciences, Inc. Dr. Abi-Dargham is a Deputy Editor for the journal *Biological Psychiatry*. All other authors report no competing interests.

8. Acknowledgements

The authors would like to thank Jaeyop Jeong, Sam R. Luceno, and Srineil Nizamabad for their contributions to fMRI preprocessing, Elizabeth Chan for assistance with data visualization, and Tram N.B. Nguyen and Dr. Benjamin A. Ely for helpful discussions. We would also like to acknowledge the substantial computing resources and technical assistance provided by Stony Brook Medicine Research Computing, with substantial support from Allen Zawada and James Xikis, as well as Stony Brook Research Computing and Cyberinfrastructure and the Institute for Advanced Computational Science at Stony Brook University for access to the high-performance SeaWulf computing system, with notable support from Fırat Coşkun, Daniel Wood, and David Carlson.

References

1. Reith J, Benkelfat C, Sherwin A, et al. Elevated dopa decarboxylase activity in living brain of patients with psychosis. *Proceedings of the National Academy of Sciences*. 1994;91(24):11651-11654. doi:10.1073/pnas.91.24.11651

2. Hietala J, Syvälahti E, Kuoppamäki M, et al. Presynaptic dopamine function in striatum of neuroleptic-naive schizophrenic patients. *The Lancet*. 1995;346(8983):1130-1131. doi:10.1016/s0140-6736(95)91801-9

3. Hietala J, Syvälahti E, Vilkman H, et al. Depressive symptoms and presynaptic dopamine function in neuroleptic-naive schizophrenia. *Schizophrenia Research*. 1999;35(1):41-50. doi:10.1016/s0920-9964(98)00113-3

4. Lindström LH, Gefvert O, Hagberg G, et al. Increased dopamine synthesis rate in medial prefrontal cortex and striatum in schizophrenia indicated by L-(β-11C) DOPA and PET. *Biological Psychiatry*. 1999;46(5):681-688. doi:10.1016/s0006-3223(99)00109-2

5. Meyer-Lindenberg A, Miletich RS, Kohn PD, et al. Reduced prefrontal activity predicts exaggerated striatal dopaminergic function in schizophrenia. *Nature Neuroscience*. 2002;5(3):267-271. doi:10.1038/nn804

6. McGowan S, Lawrence AD, Sales T, Quested D, Grasby P. Presynaptic Dopaminergic Dysfunction in Schizophrenia. *Archives of General Psychiatry*. 2004;61(2)doi:10.1001/archpsyc.61.2.134

7. Nozaki S, Kato M, Takano H, et al. Regional dopamine synthesis in patients with schizophrenia using L-[β-11C]DOPA PET. *Schizophrenia Research*. 2009;108(1-3):78-84. doi:10.1016/j.schres.2008.11.006

8. Egerton A, Chaddock CA, Winton-Brown TT, et al. Presynaptic Striatal Dopamine Dysfunction in People at Ultra-high Risk for Psychosis: Findings in a Second Cohort. *Biological Psychiatry*. 2013;74(2):106-112. doi:10.1016/j.biopsych.2012.11.017

9. Howes OD, Montgomery AJ, Asselin M-C, et al. Elevated Striatal Dopamine Function Linked to Prodromal Signs of Schizophrenia. *Archives of General Psychiatry*. 2009;66(1)doi:10.1001/archgenpsychiatry.2008.514

10. Howes OD, Bose SK, Turkheimer F, et al. Dopamine Synthesis Capacity Before Onset of Psychosis: A Prospective [18F]-DOPA PET Imaging Study. *American Journal of Psychiatry*. 2011;168(12):1311-1317. doi:10.1176/appi.ajp.2011.11010160

11. Abi-Dargham A, Gil R, Krystal J, et al. Increased striatal dopamine transmission in schizophrenia: confirmation in a second cohort. *Am J Psychiatry*. Jun 1998;155(6):761-7. doi:10.1176/ajp.155.6.761

12. Laruelle M, Abi-Dargham A, van Dyck CH, et al. Single photon emission computerized tomography imaging of amphetamine-induced dopamine release in drug-free schizophrenic subjects. *Proc Natl Acad Sci U S A*. Aug 20 1996;93(17):9235-40. doi:10.1073/pnas.93.17.9235

13. Breier A, Su TP, Saunders R, et al. Schizophrenia is associated with elevated amphetamine-induced synaptic dopamine concentrations: Evidence from a novel positron emission tomography method. *Proceedings of the National Academy of Sciences*. 1997;94(6):2569-2574. doi:10.1073/pnas.94.6.2569

14. Kegeles LS, Abi-Dargham A, Frankle WG, et al. Increased Synaptic Dopamine Function in Associative Regions of the Striatum in Schizophrenia. *Archives of General Psychiatry*. 2010;67(3)doi:10.1001/archgenpsychiatry.2010.10

15. Abi-Dargham A, Rodenhiser J, Printz D, et al. Increased baseline occupancy of D2 receptors by dopamine in schizophrenia. *Proc Natl Acad Sci U S A*. Jul 5 2000;97(14):8104-9. doi:10.1073/pnas.97.14.8104

16. Kellendonk C, Simpson EH, Polan HJ, et al. Transient and Selective Overexpression of Dopamine D2 Receptors in the Striatum Causes Persistent Abnormalities in Prefrontal Cortex Functioning. *Neuron*. 2006;49(4):603-615. doi:10.1016/j.neuron.2006.01.023

17. Lee J, Park S. Working Memory Impairments in Schizophrenia: A Meta-Analysis. *Journal of Abnormal Psychology*. 2005;114(4):599-611. doi:10.1037/0021-843x.114.4.599

18. Park S. Schizophrenics Show Spatial Working Memory Deficits. *Archives of General Psychiatry*. 1992;49(12)doi:10.1001/archpsyc.1992.01820120063009

19. Van Snellenberg JX. Working memory and long-term memory deficits in schizophrenia: Is there a common substrate? *Psychiatry Research: Neuroimaging*. 2009;174(2):89-96. doi:10.1016/j.pscychresns.2009.04.001

20. Cazorla M, de Carvalho FD, Chohan MO, et al. Dopamine D2 receptors regulate the anatomical and functional balance of basal ganglia circuitry. *Neuron*. Jan 8 2014;81(1):153-64. doi:10.1016/j.neuron.2013.10.041

21. Alexander GE, Crutcher MD, DeLong MR. Chapter 6 Basal ganglia-thalamocortical circuits: Parallel substrates for motor, oculomotor, “prefrontal” and “limbic” functions. *The Prefrontal Its Structure, Function and Cortex Pathology*. 1991:119-146. *Progress in Brain Research*.

22. Leisman G, Braun-Benjamin O, Melillo R. Cognitive-motor interactions of the basal ganglia in development. *Front Syst Neurosci*. 2014;8:16. doi:10.3389/fnsys.2014.00016

23. Wu Y, Richard S, Parent A. The organization of the striatal output system: a single-cell juxtacellular labeling study in the rat. *Neuroscience Research*. 2000;38(1):49-62. doi:10.1016/s0168-0102(00)00140-1

24. Fujiyama F, Sohn J, Nakano T, et al. Exclusive and common targets of neostriatofugal projections of rat striosome neurons: a single neuron-tracing study using a viral vector. *European Journal of Neuroscience*. 2011;33(4):668-677. doi:10.1111/j.1460-9568.2010.07564.x

25. Lévesque M, Parent A. The striatofugal fiber system in primates: A reevaluation of its organization based on single-axon tracing studies. *Proceedings of the National Academy of Sciences*. 2005;102(33):11888-11893. doi:10.1073/pnas.0502710102

26. Labouesse MA, Torres-Herraez A, Chohan MO, et al. A non-canonical striatopallidal Go pathway that supports motor control. *Nature Communications*. 2023;14(1)doi:10.1038/s41467-023-42288-1

27. Cazorla M, Shegda M, Ramesh B, Harrison NL, Kellendonk C. Striatal D2 Receptors Regulate Dendritic Morphology of Medium Spiny Neurons via Kir2 Channels. *The Journal of Neuroscience*. 2012;32(7):2398-2409. doi:10.1523/jneurosci.6056-11.2012

28. Haber SN, Kim K-S, Mailly P, Calzavara R. Reward-Related Cortical Inputs Define a Large Striatal Region in Primates That Interface with Associative Cortical Connections, Providing a Substrate for Incentive-Based Learning. *The Journal of Neuroscience*. 2006;26(32):8368-8376. doi:10.1523/jneurosci.0271-06.2006

29. Howes OD, Kambeitz J, Kim E, et al. The Nature of Dopamine Dysfunction in Schizophrenia and What This Means for Treatment. *Archives of General Psychiatry*. 2012;69(8)doi:10.1001/archgenpsychiatry.2012.169

30. Caravaggio F, Nakajima S, Borlido C, et al. Estimating Endogenous Dopamine Levels at D2 and D3 Receptors in Humans using the Agonist Radiotracer [11C]-(+)-PHNO. *Neuropsychopharmacology*. 2014;39(12):2769-2776. doi:10.1038/npp.2014.125

31. Logothetis NK. What we can do and what we cannot do with fMRI. *Nature*. 2008;453(7197):869-878. doi:10.1038/nature06976

32. Jueptner M, Weiller C. Review: Does Measurement of Regional Cerebral Blood Flow Reflect Synaptic Activity?—Implications for PET and fMRI. *NeuroImage*. 1995;2(2):148-156. doi:10.1006/nimg.1995.1017

33. Kreitzer AC. Physiology and Pharmacology of Striatal Neurons. *Annual Review of Neuroscience*. 2009;32(1):127-147. doi:10.1146/annurev.neuro.051508.135422

34. Molchanova SM, Comhair J, Karadurmus D, et al. Tonically Active α2 Subunit-Containing Glycine Receptors Regulate the Excitability of Striatal Medium Spiny Neurons. *Frontiers in Molecular Neuroscience*. 2018;10doi:10.3389/fnmol.2017.00442

35. Van Snellenberg JX, Slifstein M, Read C, et al. Dynamic shifts in brain network activation during supracapacity working memory task performance. *Human Brain Mapping*. 2015;36(4):1245-1264. doi:10.1002/hbm.22699

36. Smith SM, Miller KL, Salimi-Khorshidi G, et al. Network modelling methods for FMRI. *NeuroImage*. 2011;54(2):875-891. doi:10.1016/j.neuroimage.2010.08.063

37. Marrelec G, Krainik A, Duffau H, et al. Partial correlation for functional brain interactivity investigation in functional MRI. *NeuroImage*. 2006;32(1):228-237. doi:10.1016/j.neuroimage.2005.12.057

38. Salvador R, Suckling J, Coleman MR, Pickard JD, Menon D, Bullmore E. Neurophysiological Architecture of Functional Magnetic Resonance Images of Human Brain. *Cerebral Cortex*. 2005;15(9):1332-1342. doi:10.1093/cercor/bhi016

39. Cassidy CM, Zucca FA, Girgis RR, et al. Neuromelanin-sensitive MRI as a noninvasive proxy measure of dopamine function in the human brain. *Proceedings of the National Academy of Sciences*. 2019;116(11):5108-5117. doi:10.1073/pnas.1807983116

40. Wengler K, Baker SC, Velikovskaya A, et al. Generalizability and Out-of-Sample Predictive Ability of Associations Between Neuromelanin-Sensitive Magnetic Resonance Imaging and Psychosis in Antipsychotic-Free Individuals. *JAMA Psychiatry*. 2024;81(2)doi:10.1001/jamapsychiatry.2023.4305

41. Gallezot J-D, Zheng M-Q, Lim K, et al. Parametric Imaging and Test–Retest Variability of 11C-(+)-PHNO Binding to D2/D3 Dopamine Receptors in Humans on the High-Resolution Research Tomograph PET Scanner. *Journal of Nuclear Medicine*. 2014;55(6):960-966. doi:10.2967/jnumed.113.132928

42. Rabiner EA, Laruelle M. Imaging the D3 receptor in humans in vivo using [11C](+)-PHNO positron emission tomography (PET). *The International Journal of Neuropsychopharmacology*. 2010;13(03)doi:10.1017/s1461145710000088

43. Williams JC, Tubiolo PN, Gil RB, et al. Auditory and Visual Thalamocortical Connectivity Alterations in Unmedicated People with Schizophrenia: An Individualized Sensory Thalamic Localization and Resting-State Functional Connectivity Study. *medRxiv*. 2024:2024.12.18.24319241. doi:10.1101/2024.12.18.24319241

44. Van Snellenberg JX, Conway ARA, Spicer J, Read C, Smith EE. Capacity estimates in working memory: Reliability and interrelationships among tasks. *Cognitive, Affective, & Behavioral Neuroscience*. 2014;14(1):106-116. doi:10.3758/s13415-013-0235-x

45. Van Snellenberg JX, Girgis RR, Horga G, et al. Mechanisms of Working Memory Impairment in Schizophrenia. *Biological Psychiatry*. 2016;80(8):617-626. doi:10.1016/j.biopsych.2016.02.017

46. Gratton C, Laumann TO, Nielsen AN, et al. Functional Brain Networks Are Dominated by Stable Group and Individual Factors, Not Cognitive or Daily Variation. *Neuron*. 2018;98(2):439-452.e5. doi:10.1016/j.neuron.2018.03.035

47. Elliott ML, Knodt AR, Cooke M, et al. General functional connectivity: Shared features of resting-state and task fMRI drive reliable and heritable individual differences in functional brain networks. *Neuroimage*. Apr 1 2019;189:516-532. doi:10.1016/j.neuroimage.2019.01.068

48. Glasser MF, Sotiropoulos SN, Wilson JA, et al. The minimal preprocessing pipelines for the Human Connectome Project. *NeuroImage*. 2013;80:105-124. doi:10.1016/j.neuroimage.2013.04.127

49. Williams JC, Tubiolo PN, Luceno JR, Van Snellenberg JX. Advancing motion denoising of multiband resting-state functional connectivity fMRI data. *NeuroImage*. 2022;249doi:10.1016/j.neuroimage.2022.118907

50. Fair DA, Schlaggar BL, Cohen AL, et al. A method for using blocked and event-related fMRI data to study “resting state” functional connectivity. *NeuroImage*. 2007;35(1):396-405. doi:10.1016/j.neuroimage.2006.11.051

51. Kay SR, Fiszbein A, Opler LA. The positive and negative syndrome scale (PANSS) for schizophrenia. *Schizophr Bull*. 1987;13(2):261-76. doi:10.1093/schbul/13.2.261

52. van de Giessen E, Weinstein JJ, Cassidy CM, et al. Deficits in striatal dopamine release in cannabis dependence. *Mol Psychiatry*. Jan 2017;22(1):68-75. doi:10.1038/mp.2016.21

53. Hedges LV. Distribution Theory for Glass's Estimator of Effect Size and Related Estimators. *Journal of Educational Statistics*. 1981;6(2)doi:10.2307/1164588

54. Kline RB. *Beyond significance testing: Statistics reform in the behavioral sciences (2nd ed.)*. 2013.

55. Šidák Z. Rectangular Confidence Regions for the Means of Multivariate Normal Distributions. *Journal of the American Statistical Association*. 1967;62(318):626-633. doi:10.1080/01621459.1967.10482935

56. Benjamini Y, Hochberg Y. Controlling the False Discovery Rate: A Practical and Powerful Approach to Multiple Testing. *Journal of the Royal Statistical Society: Series B (Methodological)*. 2018;57(1):289-300. doi:10.1111/j.2517-6161.1995.tb02031.x

57. Simpson EH, Kellendonk C. Insights About Striatal Circuit Function and Schizophrenia From a Mouse Model of Dopamine D2 Receptor Upregulation. *Biological Psychiatry*. 2017;81(1):21-30. doi:10.1016/j.biopsych.2016.07.004

58. Simpson EH, Kellendonk C, Kandel E. A possible role for the striatum in the pathogenesis of the cognitive symptoms of schizophrenia. *Neuron*. Mar 11 2010;65(5):585-96. doi:10.1016/j.neuron.2010.02.014

59. Chen X, Huddleston DE, Langley J, et al. Simultaneous imaging of locus coeruleus and substantia nigra with a quantitative neuromelanin MRI approach. *Magnetic Resonance Imaging*. 2014;32(10):1301-1306. doi:10.1016/j.mri.2014.07.003

60. Zucca FA, Vanna R, Cupaioli FA, et al. Neuromelanin organelles are specialized autolysosomes that accumulate undegraded proteins and lipids in aging human brain and are likely involved in Parkinson's disease. *npj Parkinson's Disease*. 2018;4(1)doi:10.1038/s41531-018-0050-8

61. van der Pluijm M, Wengler K, Reijers PN, et al. Neuromelanin-Sensitive MRI as Candidate Marker for Treatment Resistance in First-Episode Schizophrenia. *American Journal of Psychiatry*. 2024;181(6):512-519. doi:10.1176/appi.ajp.20220780

62. Vano LJ, McCutcheon RA, Rutigliano G, et al. Mesostriatal Dopaminergic Circuit Dysfunction in Schizophrenia: A Multimodal Neuromelanin-Sensitive Magnetic Resonance Imaging and [18F]-DOPA Positron Emission Tomography Study. *Biological Psychiatry*. 2024;96(8):674-683. doi:10.1016/j.biopsych.2024.06.013

63. Horga G, Cassidy CM, Xu X, et al. Dopamine-Related Disruption of Functional Topography of Striatal Connections in Unmedicated Patients With Schizophrenia. *JAMA Psychiatry*. Aug 1 2016;73(8):862-70. doi:10.1001/jamapsychiatry.2016.0178

64. McCutcheon RA, Abi-Dargham A, Howes OD. Schizophrenia, Dopamine and the Striatum: From Biology to Symptoms. *Trends in Neurosciences*. 2019;42(3):205-220. doi:10.1016/j.tins.2018.12.004

65. Weinstein JJ, Chohan MO, Slifstein M, Kegeles LS, Moore H, Abi-Dargham A. Pathway-Specific Dopamine Abnormalities in Schizophrenia. *Biological Psychiatry*. 2017;81(1):31-42. doi:10.1016/j.biopsych.2016.03.2104

66. Abi-Dargham A, Javitch JA, Slifstein M, et al. Dopamine D1R Receptor Stimulation as a Mechanistic Pro-cognitive Target for Schizophrenia. *Schizophrenia Bulletin*. 2022;48(1):199-210. doi:10.1093/schbul/sbab095

67. Cools R, D'Esposito M. Inverted-U–Shaped Dopamine Actions on Human Working Memory and Cognitive Control. *Biological Psychiatry*. 2011;69(12):e113-e125. doi:10.1016/j.biopsych.2011.03.028

68. Duvarci S, Simpson EH, Schneider G, Kandel ER, Roeper J, Sigurdsson T. Impaired recruitment of dopamine neurons during working memory in mice with striatal D2 receptor overexpression. *Nature Communications*. 2018;9(1)doi:10.1038/s41467-018-05214-4

69. Krabbe S, Duda J, Schiemann J, et al. Increased dopamine D2 receptor activity in the striatum alters the firing pattern of dopamine neurons in the ventral tegmental area. *Proceedings of the National Academy of Sciences*. 2015;112(12)doi:10.1073/pnas.1500450112

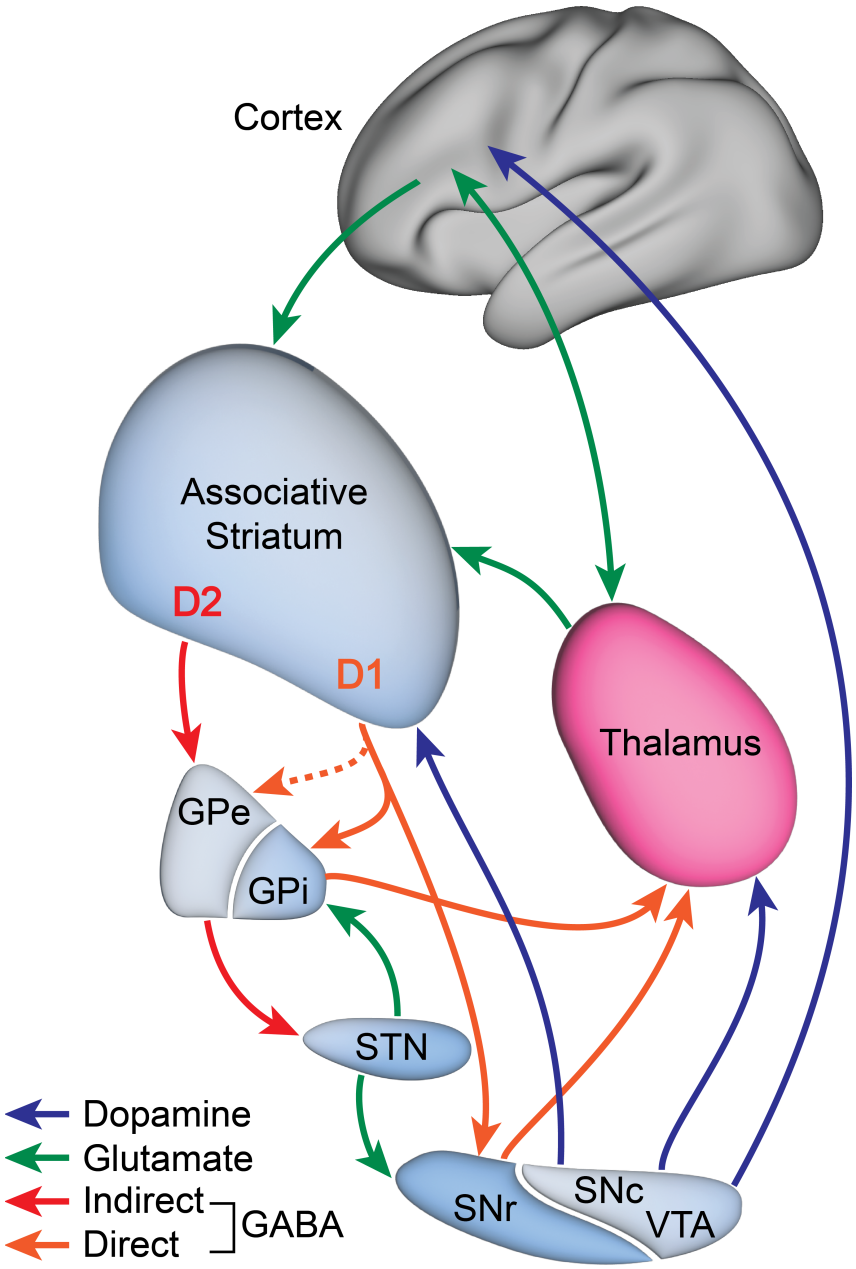

Figure 1. Schematic of basal ganglia-thalamo-cortical circuitry, highlighting glutamatergic (green arrows), GABAergic (red and orange arrows), and dopaminergic (blue arrows) connections between regions. Orange dashed line represents bridging collateral axonal projections from the associative striatum (primarily dorsal caudate) to the globus pallidus externus (GPe). GPi = globus pallidus internus; STN = subthalamic nucleus; SNr = substantia nigra pars reticulata; SNc = substantia nigra pars compacta; VTA = ventral tegmental area.

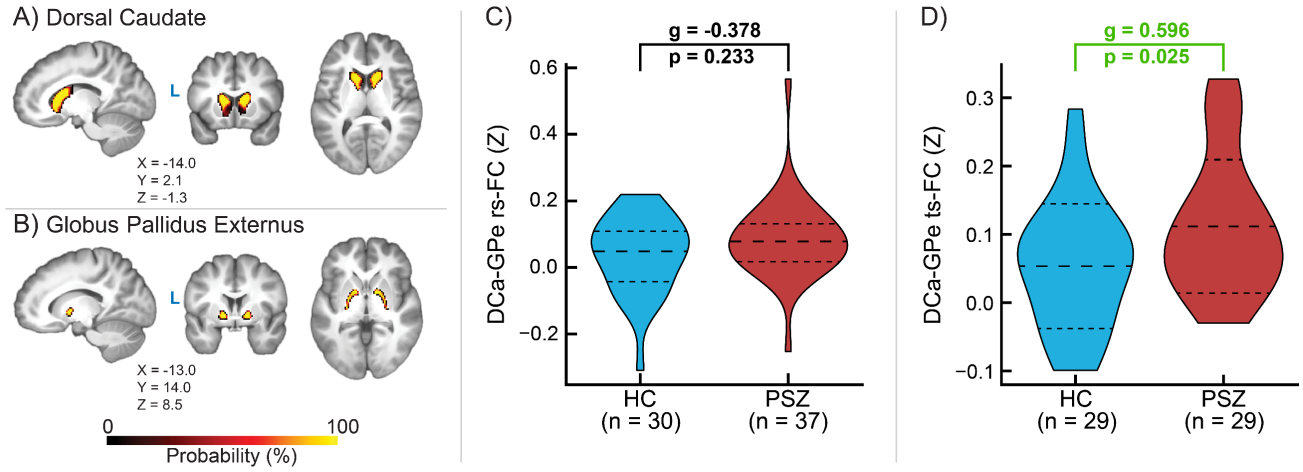

Figure 2. Probability density of A) dorsal caudate (DCa) and B) globus pallidus externus (GPe) regions of interest in the task-based fMRI sample (N = 58), as well as group differences in DCa-GPe resting-state functional connectivity (rs-FC; panel C) and task-state functional connectivity (ts-FC; panel D) between healthy controls (HC) and persons with schizophrenia (PSZ). Long-dashed and short-dashed lines denote median and interquartile range in panel C (due to non-normal data) and means and standard deviations in panel D. FC was calculated controlling for the average timeseries in dorsolateral prefrontal cortex, globus pallidus internus, substantia nigra, and mediodorsal nucleus.

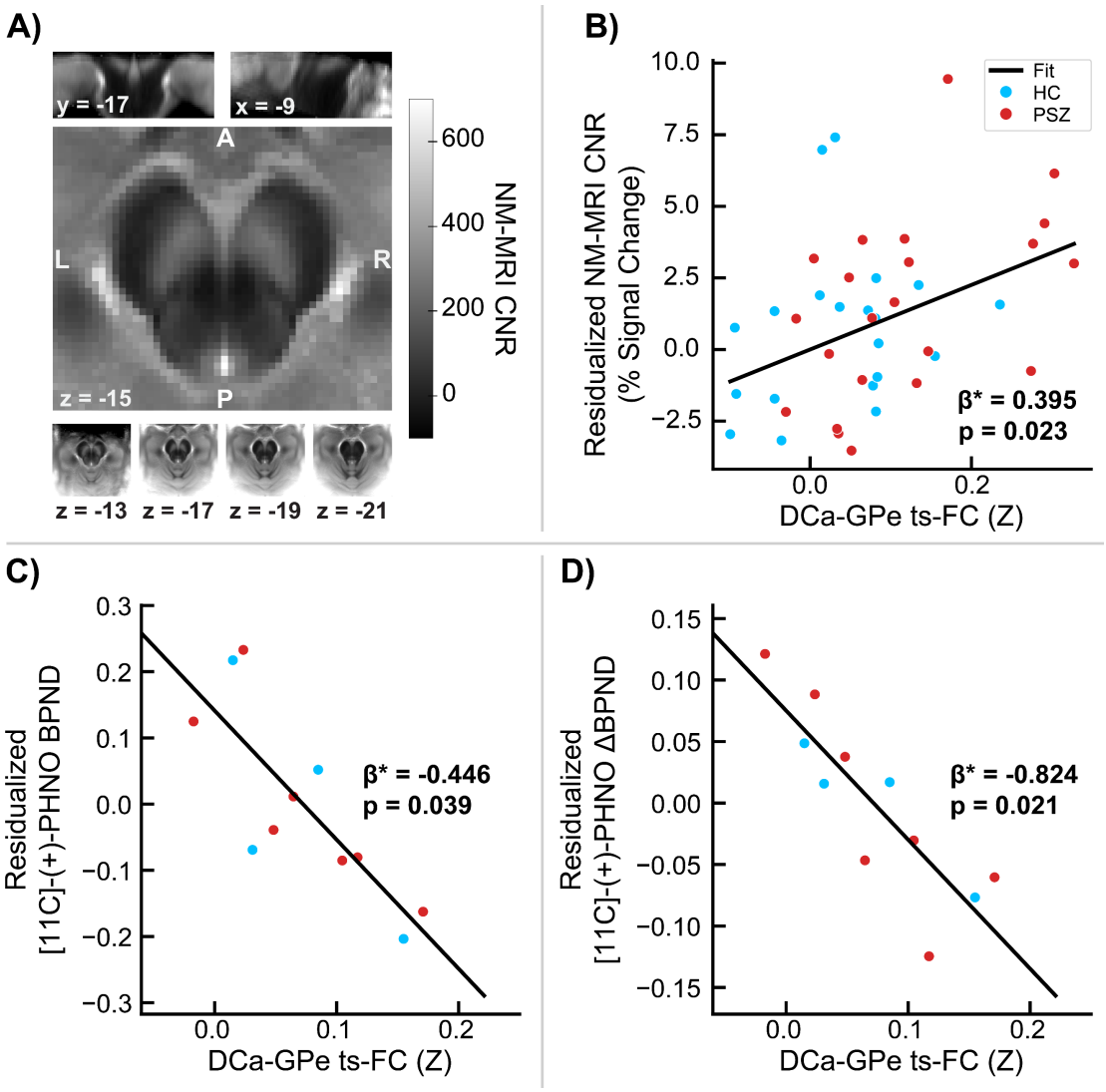

Figure 3. A) Average neuromelanin-sensitive MRI (NM-MRI) contrast-to-noise ratio (CNR) across all participants (N = 42). B) Association between average NM-MRI CNR in the voxels shown in panel A and task-state functional connectivity (ts-FC) between dorsal caudate (DCa) and globus pallidus externus (GPe), controlling for age, biological sex, and diagnosis. Associations between C) [^{11}C]-(+)-PHNO Baseline BPND or D) ΔBPND following amphetamine challenge and DCa-GPe ts-FC controlling for age, biological sex, and diagnosis. Regression plot inlay shows standardized regression coefficient β*.

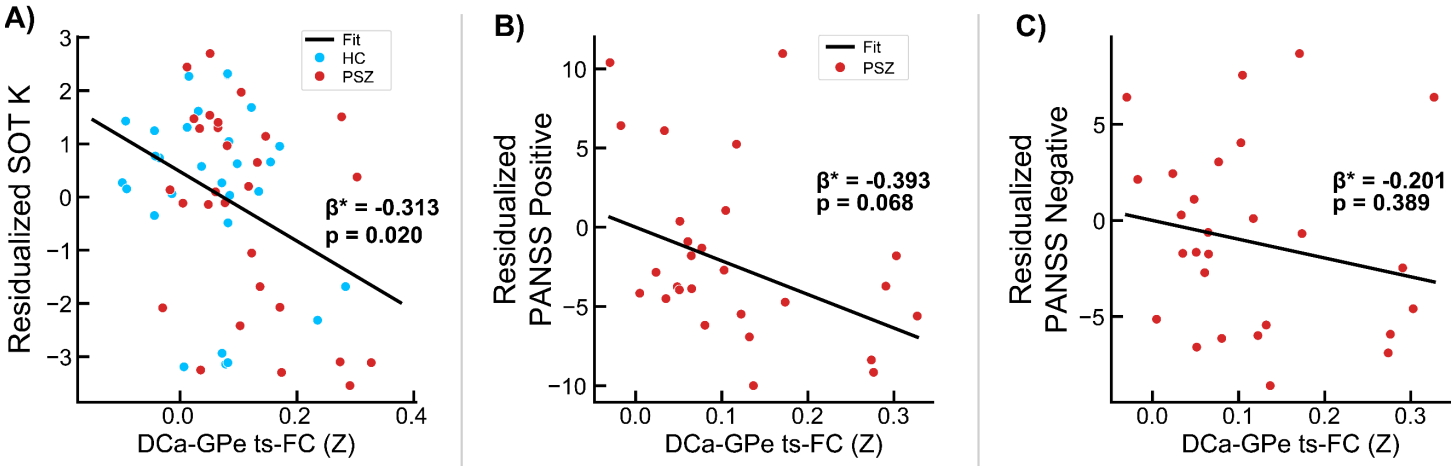

Figure 4. Associations between working memory capacity *K* calculated from self-ordered working memory task (SOT) performance (panel A), Positive and Negative Syndrome Scale (PANSS) positive symptom score (panel B), or PANSS negative symptom score (panel C), and task-state functional connectivity (ts-FC) between dorsal caudate (DCa) and globus pallidus externus (GPe). Associations between *K* and DCa-GPe ts-FC were calculated in all participants (N = 58) controlling for age, biological sex, and diagnosis, while PANSS symptom associations were calculated in persons with schizophrenia (PSZ) only, controlling for age and biological sex. Plot inlays shows standardized regression coefficient β*.

Table 1. Participant Demographics and Clinical Measures

Participant Characteristic	Task-Based (N = 58)			Resting State (N = 67)		
	PSZ (n = 29)	HC (n = 29)	Effect Size[a]	PSZ (n = 37)	HC (n = 30)	Effect Size[a]
Functional Magnetic Resonance Imaging Datasets						
Age, Years (SD)	33.4 (12.7)	32.4 (9.7)	-0.086	32.7 (12.7)	32.5 (9.7)	-0.015
Biological Sex, Female (%)	9.0 (31.0%)	9.0 (31.0%)	0.0	11.0 (29.7%)	8.0 (26.7%)	0.034
Ethnicity, Hispanic (%)	7.0 (24.1%)	8.0 (27.6%)	-0.038	9.0 (24.3%)	8.0 (26.7%)	0.033
Race			0.311			0.219
African American (%)	14.0 (48.3%)	13.0 (44.8%)		18.0 (48.6%)	13.0 (43.3%)	
Asian (%)	3.0 (10.3%)	3.0 (10.3%)		3.0 (8.1%)	3.0 (10.0%)	
Caucasian (%)	6.0 (20.7%)	8.0 (27.6%)		9.0 (24.3%)	9.0 (30.0%)	
More than one (%)	4.0 (13.8%)	0.0 (0.0%)		3.0 (8.1%)	0.0 (0.0%)	
Other (%)	2.0 (6.9%)	5.0 (17.2%)		4.0 (10.8%)	5.0 (16.7%)	
Handedness[b]			0.189			0.195
Ambidextrous (%)	0.0 (0.0%)	0.0 (0.0%)		0.0 (0.0%)	0.0 (0.0%)	
Left (%)	0.0 (0.0%)	2.0 (6.9%)		0.0 (0.0%)	2.0 (6.7%)	
Right (%)	29.0 (100.0%)	27.0 (93.1%)		37.0 (100.0%)	28.0 (93.3%)	
Smoker[c,d] (%)	9.0 (31.0%)	3.0 (10.3%)	-0.510	11.0 (29.7%)	3.0 (10.0%)	-0.433
Parental SES[e,f] (SD)	40.3 (13.9)	44.7 (11.2)	0.345	38.6 (14.3)	44.6 (11.0)	0.455
PANSS Total[g] (SD)	61.6 (18.3)	33.0 (4.8)	-2.03*	65.3 (18.0)	32.4 (2.9)	-2.348*
PANSS General[g] (SD)	31.4 (9.9)	17.0 (2.4)	-1.886*	33.2 (9.8)	16.7 (1.5)	-2.163*
PANSS Negative[g] (SD)	14.4 (4.8)	8.9 (2.7)	-1.341*	15.5 (5.3)	8.6 (2.3)	-1.560*
PANSS Positive[g] (SD)	15.9 (5.4)	7.2 (0.46)	-2.177*	16.6 (5.2)	7.1 (0.27)	-2.372*
CDRS[h] (SD)	3.1 (3.9)	0.17 (0.69)	-0.938*	3.7 (4.2)	0.17 (0.69)	-1.036*
AP Medication-Naïve[k] (%)	14 (48.3%)	—	—	19 (51.4%)	—	—
	Positron Emission Tomography Dataset			***Neuromelanin-Sensitive MRI Dataset***		
	PSZ (n = 7)	HC (n = 4)	Effect Size[a]	PSZ (n = 22)	HC (n = 20)	Effect Size[a]
Age, Years (SD)	23.1 (6.3)	31.5 (11.9)	0.888	35.1 (13.9)	29.4 (8.5)	-0.479
Biological Sex, Female (%)	4 (57.1%)	1 (25.0%)	0.311	8 (36.4%)	7 (35.0%)	0.014
Ethnicity, Hispanic (%)	0 (0.0%)	1 (25.0%)	0.646	4 (18.2%)	7 (35.0%)	0.236
Race			0.516			0.375
African American (%)	3 (42.9%)	2 (50.0%)		12 (54.5%)	8 (40.0%)	
Asian (%)	2 (28.6%)	0 (0.0%)		2 (9.1%)	2 (10.0%)	
Caucasian (%)	2 (28.6%)	1 (25.0%)		4 (18.2%)	6 (30.0%)	
More than one (%)	0 (0.0%)	0 (0.0%)		3 (13.6%)	0 (0.0%)	
Other (%)	0 (0.0%)	1 (25.0%)		1 (4.6%)	4 (20.0%)	
Handedness[b]			0.418			0.235
Ambidextrous (%)	0 (0.0%)	0 (0.0%)		0 (0.0%)	0 (0.0%)	
Left (%)	0 (0.0%)	1 (25.0%)		0 (0.0%)	2 (10.0%)	
Right (%)	7 (100.0%)	3 (75.0%)		22 (100.0%)	18 (90.0%)	
Smoker[c] (%)	2 (28.6%)	0 (0.0%)	-0.400			
Parental SES[e,f] (SD)	46.8 (15.8)	34.6 (5.9)	-0.835	42.1 (13.4)	45.7 (10.2)	0.287
PANSS Total[g] (SD)	78.6 (21.5)	33.5 (4.5)	-2.316*	64.4 (19.3)	32.8 (3.1)	-2.163*
PANSS General (SD)	39.7 (14.3)	17.8 (2.9)	-1.699*	32.8 (10.6)	16.6 (1.5)	-2.030*
PANSS Negative (SD)	19.1 (3.8)	8.8 (1.7)	-2.914*	14.8 (5.1)	9.1 (2.6)	-1.342*
PANSS Positive (SD)	19.7 (5.6)	7.0 (0)	-2.519*	16.9 (5.7)	7.1 (0.3)	-2.291*
CDRS[h] (SD)	6.4 (5.3)	0.8 (1.5)	-1.179	3.4 (4.2)	0.2 (0.8)	-0.977*
AP Medication-Naïve[k] (%)	7 (100%)	—	—	11 (50.0%)	—	—

[a]Effect sizes for continuous variables were calculated with Hedges's g; effect sizes for dichotomous and categorical variables were calculated with Cramér's V.
[b]Handedness was reported using the Edinburgh Handedness Inventory.
[c]Smoking status defined as current daily nicotine use.
[d]Smoking status was unavailable for 2 participants (1 PSZ and 1 HC) from the resting-state sample and 1 HC from the task-based sample.
[e]Mean Parental SES was reported using the Hollingshead Four Factor Index Scale of Socioeconomic Status scale.
[f]Parental SES data were unavailable for 7 participants (5 PSZ and 2 HC) from the resting-state sample, 4 participants (2 PSZ and 2 HC) from the task-based sample, and 2 HC from the neuromelanin-sensitive MRI sample.
[g]PANSS data were unavailable for 8 participants (4 PSZ and 4 HC) from the resting-state sample, 6 participants (2 PSZ and 4 HC) from the task-based sample, and 3 participants (1 PSZ and 2 HC) from the neuromelanin-sensitive MRI sample.
[h]CDRS data were unavailable for 22 participants (10 PSZ and 12 HC) in the resting-state sample, 16 participants (5 PSZ and 11 HC) in the task-based sample, and 6 participants (2 PSZ and 4 HC) in the neuromelanin-sensitive MRI sample.

[k]All PSZ in this study were antipsychotic-free, defined as no exposure to oral antipsychotic medication for at least 3 weeks, and no exposure to intramuscular antipsychotic medications for at least 6 months, prior to study participation. PSZ were considered to be medication-naïve if they had fewer than 2 weeks of cumulative lifetime exposure to antipsychotic medications.
*Asterisks indicate $p < 0.05$ (uncorrected), as determined using Mann-Whitney U-tests.

Abbreviations: PSZ: People with Schizophrenia; HC: Healthy Controls; SD: standard deviation; SES: socioeconomic status; PANSS: Positive and Negative Syndrome Scale; CDRS: Calgary Depression Scale for Schizophrenia; AP: Antipsychotic.